perature, using a tensile tester and a strain rate of 5 mm min^{-1}. Five samples were tested for each specimen. The results obtained from these experiments were within 15 % assuring good statistics.

Received: October 24, 2003
Final version: April 8, 2004

[1] P. Maiti, P. H. Nam, M. Okamoto, N. Hasegawa, A. Usuki, *Macromolecules* **2002**, *35*, 2042.
[2] P. Maiti, P., M. Okamoto, *Macromol. Mater. Eng.* **2003**, *288*, 440.
[3] L. Priya, J. P. Jog, *J. Polym Sci., Part B: Polym. Phys.* **2002**, *40*, 1682.
[4] L. Priya, J. P. Jog, *J. Polym Sci., Part B: Polym. Phys.* **2003**, *41*, 31.
[5] Q. Wu, X. Liu, L. A. Berglund, *Macromol. Rapid Commun.* **2001**, *22*, 1438.
[6] L. J. Mathias, R. D. Davis, W. L. Jarrett, *Macromolecules* **1999**, *32*, 7958.
[7] D. L. Van der Hart, A. Asano, J. W. Gilman, *Chem. Mater.* **2001**, *13*, 3781.
[8] Q. M. Zhang, H. Li, M. Poh, F. Xia, Z. Y. Cheng, H. Xu, C. Huang, *Nature* **2002**, *419*, 284.
[9] Q. M. Zhang, V. Bharti, X. Zhao, *Science* **1998**, *280*, 2101.
[10] H. Xu, Z. Y. Cheng, D. Olson, T. Mai, Q. M. Zhang, *Appl. Phys. Lett.* **2001**, *78*, 2360.
[11] P. C. A. Hammes, P. P. L. Regtien, *Sens. Actuators, A* **1992**, *32*, 396.
[12] G. Guerra, F. E. Karasz, W. J. MacKnight, *Macromolecules* **1986**, *19*, 1935.
[13] R. Miller, *J. Polym. Sci., Polym. Chem. Ed.* **1976**, *14*, 2325.
[14] J. Scheinbeim, C. Nakafuku, B. A. Newman, K. D. Pae, *J. Appl. Phys.* **1979**, *50*, 4399.
[15] A. J. Lovinger, *Polymer* **1981**, *22*, 412.
[16] J. Wang, H. Li, J. Liu, Y. Duan, S. Jiang, S. Yan, *J. Am. Chem. Soc.* **2003**, *125*, 1496.
[17] R. A. Vaia, H. Ishii, E. P. Giannelis, *Chem. Mater.* **1993**, *5*, 1694.
[18] B. K. G. Theng, *Formation and Properties of Clay-Polymer Complexes*, Vol. 9, Elsevier, Amsterdam **1979**.
[19] M. Kobayashi, K. Tashiro, H. Tadokoro, *Macromolecules* **1975**, *8*, 158.
[20] Y. Takahashi, Y. Matsubara, H. Tadokoro, *Macromolecules* **1982**, *15*, 334.
[21] F. L. Binsbergen, B. G. M. de Lange, *Polymer* **1968**, *9*, 23.
[22] W. M. Prest, Jr., D. J. Luca, *J. Appl. Phys.* **1978**, *49*, 5042.
[23] L. E. Nielson, *J. Appl. Polym. Sci.* **1966**, *10*, 97.
[24] S. Lanceros-Mendez, J. F. Mano, A. M. Costa, V. H. Schmidt, *J. Macromol. Sci. Phys.* **2001**, *B40*, 517.
[25] D. Gersappe, *Phys. Rev. Lett.* **2002**, *89*, 058 301.

Molecular-Level Insulation: An Approach to Controlling Interfacial Charge Transfer**

By *Saif A. Haque**, *Jong S. Park*, *Mohan Srinivasarao*, and *James R. Durrant*

The immobilization of redox-active or photo-active molecules on semiconductor surfaces is fundamentally important for the development of molecular electronic devices, including solar cells, biological and chemical sensors, and heterosupramolecular systems.[1–5] One such area of research attracting particular interest at present is the functionalization of nanocrystalline metal oxide films by the adsorption of molecular dyes. Such functionalized metal oxide films are currently under investigation for device applications ranging from dye-sensitized solar cells to electrochromic displays. The attachment of molecular dyes to the metal oxide nanoparticles is typically achieved via acidic groups, such as carboxylates or sulfonates, covalently attached to the sensitizer dye. Such acid groups have been shown to form ester-type linkages to metal oxide electrodes.[6] This attachment strategy is however limited to the use of dyes with suitable acidic groups, precluding the use of most commercially available molecular dyes. Moreover such direct covalent attachment can often result in unnecessarily strong electronic interactions between the molecular dye and the metal oxide electrode. This has been particularly observed for small organic dyes, where direct covalent attachment to the electrode surface as been shown to result in undesirably fast interfacial recombination of photogenerated charge-separated species,[7,8] limiting practical device applications.

In this paper we present an alternative strategy to the immobilization of molecular dyes on nanocrystalline TiO_2 electrodes. Our strategy is based upon insulated sensitizer dyes, in which the dye molecule is encapsulated at the molecular level by a cyclodextrin macrocycle, limiting the interaction between the TiO_2 semiconductor surface and dye molecule and there-

[*] Dr. S. A. Haque, Dr. J. R. Durrant
Department of Chemistry, Centre for Electronic Materials and Devices
Imperial College of Science Technology and Medicine
London SW7 2AZ (UK)
E-mail: s.a.haque@imperial.ac.uk
J. S. Park, Dr. M. Srinivasarao
School of Textile and Fiber Engineering and
School of Chemistry and Biochemistry, Georgia Institute of Technology
Atlanta, GA 30332 (USA)

[**] This work was supported by the Engineering and Physical Sciences Research Council (EPSRC). M. S. would like to thank a grant through the National Textile Center grant (Department of Commerce) and the National Science Foundation (DMR-096240, CAREER) for financial support. We would also like to thank Emilio Palomares for helpful discussions and Alex Green for synthesis of the TiO_2 nanoparticles. Supporting Information is available online from Wiley Interscience or from the author.

 DOI: 10.1002/adma.200400327

ADVANCED MATERIALS

by allowing control of interfacial charge recombination. Encapsulation of molecular dyes, or indeed, polymers provides an attractive approach to control the intermolecular interactions and can also lead to enhanced chemical and photo stability, redox reversibility, and enhanced fluorescence and electroluminescence efficiency.[9–15] We have employed azobenzene based dyes that are threaded by cyclodextrin (CD) macrocycles and then capped by bulky end groups to prevent de-threading of the CD ring. The cyclodextrin macrocycles have two functions: i) a hydrophobic inner cavity serving as a protective sheath around the dye and a barrier to charge recombination and ii) the hydrophilic outer surface of the CD providing functional components for dye adsorption on a nanocrystalline TiO_2 film. Herein we demonstrate that such cyclodextrin threaded sensitizer dye rotaxanes can be used to functionalize nanocrystalline TiO_2, resulting in a long-lived photogenerated charge separation.

The chemical structure of the azobenzene dye rotaxane is shown in Figure 1 (dye **3**). The dye was synthesized following a modified version of a previously published procedure,[16,17] by a diazotization reaction of 4,4′-diaminoazobenzene (the 'thread') in the presence of α-cyclodextrin **4** in water. This was followed by a further, coupling reaction with *N*,*N*-dimethyl-1-naphthylamine (the 'capping groups') at both ends of

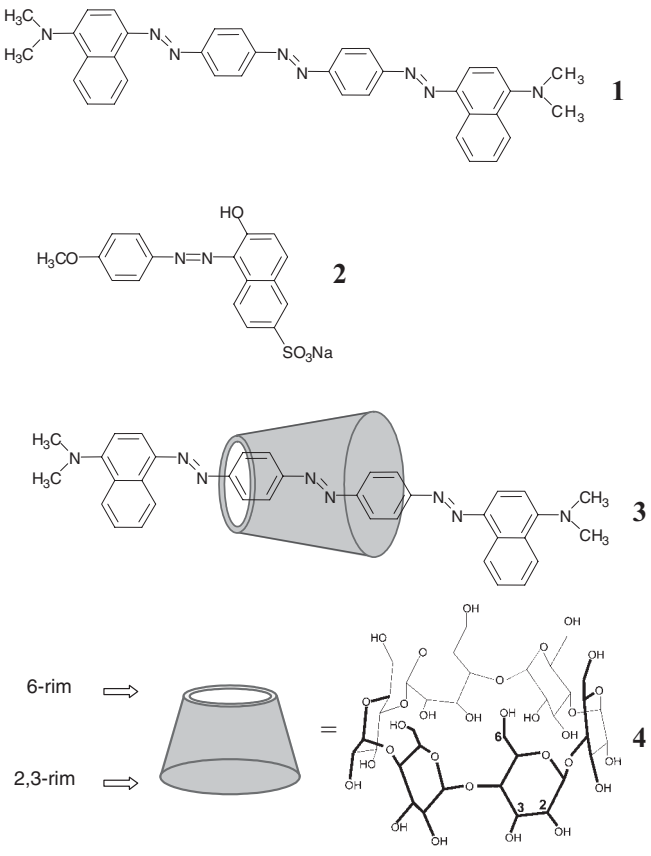

Figure 1. Shows the chemical structure of the azo-benzene-based sensitizer dyes studied here. Also shown is the structure of the α-cyclodextrin macrocycle **4** employed to encapsulate the sensitizer dye.

chromophore. For comparison, the free dye (dye **1**) was synthesized following the same procedure in the absence of α-cyclodextrin. The formation of rotaxane structure was fully characterized using 1H NMR and 2D correlation spectroscopy (COSY) techniques (see Supplementary information). Full details of the synthesis and characterization of the dye will be given elsewhere.

We consider first the attachment of the dyes to nanocrystalline TiO_2. Nanocrystalline TiO_2 films were prepared on glass substrates from an aqueous suspension of 15 nm TiO_2 colloids following a previously published procedure.[18] Dye adsorption was achieved by immersion of the TiO_2 film in 0.1 mM solutions of dyes **1** and **3** in tetrahydrofuran (THF) at 25 °C for 8 h, followed by rinsing with neat THF to remove any loosely adsorbed dye. Figure 2 shows the steady-state UV-vis

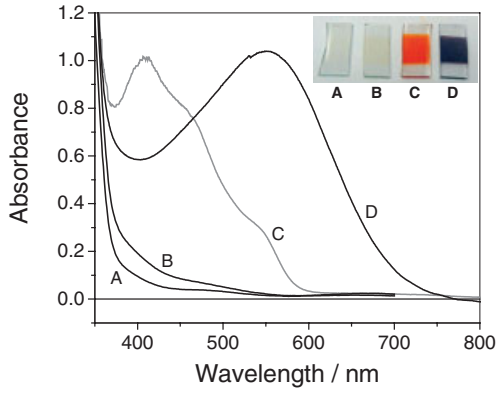

Figure 2. Steady-state UV-vis absorption spectra of nanocrystalline TiO_2 films sensitized with dyes **1** (curve B), **2** (curve C), and **3** (curve D), respectively. Also shown is the absorption spectrum of a bare, unsensitized nanocrystalline TiO_2 film (curve A). Inset shows the corresponding images of sensitized films.

absorption spectra obtained for dye **1**/TiO_2 and dye **3**/TiO_2 nanocrystalline films (spectra B and D, respectively). Also shown are the absorption spectra of a bare TiO_2 film prior to any dye adsorption (spectrum A) and a further control sample dye **2**/TiO_2 employed in this study (spectrum C), which incorporates a sulfonate group to achieve direct binding to the TiO_2 film.

Bare TiO_2 films (Fig. 2, spectrum A) are transparent and colorless in the visible region, showing a characteristic absorption increase below ~400 nm due to the onset of TiO_2 band-gap excitation. Immersion of the TiO_2 film in THF solution of dye **1** results in little or no adsorption of this dye as indicated in Figure 2, curve B. In contrast we find that the rotaxanated dye **3** adsorbs very well on the nanocrystalline TiO_2 film, resulting in a deep red–purple coloration of the film, with an absorption maximum at 550 nm, as indicated in Figure 2, inset D, indistinguishable from the absorption maximum of this dye in solution. These observations demonstrate the presence of a strong interaction between the CD macrocycle and the TiO_2 nanoparticle surface. Employing an extinction coefficient of 44 000 $M^{-1}\,cm^{-1}$ at 550 nm for dye **3**, we obtained a loading of

24 nmol on the ~3 μm thick TiO_2 film (1 cm^2 macroscopic area); corresponding to surface coverage of ~0.75 ± 0.10 monolayers (assuming a dye cross-sectional area of 230 $Å^2$). We note that following adsorption of dye **3**, the sensitized film was remarkably stable, with subsequent rinsing and washing in THF resulting in no apparent desorption of the dye. We attribute this strong, approximately monolayer coverage to a favorable interaction between the hydrophilic –OH groups on the outer surface of the CD macrocycle and the hydrophilic TiO_2 nanoparticle surface.

We turn now to interfacial charge transfer kinetics observed for the dye-sensitized nanocrystalline TiO_2 films. Microsecond–millisecond transient-absorption spectroscopy was employed to monitor the charge-recombination dynamics following photoexcitation of the dye. Details of the transient-absorption apparatus have been described previously.[19–21] Our transient-absorption studies employed two dyes **2** and **3** as illustrated in Figure 1. Both dyes have the same structural chromophore (azobenzene unit) but differ in mechanism of attachment to the TiO_2 surface. For dye **2** binding is achieved by direct binding employing the acidic sulfonate linkage $–SO_3H$, whereas for dye **3** binding is achieved indirectly through –OH groups on outside of the CD. Both sensitized films of dyes **2** and **3** were covered in 200 μL of redox inert electrolyte (anhydrous 0.3 M lithium trifluoromethane sulfonate in propylene carbonate) followed by a glass cover-slip. All transient-absorption experiments were conducted at 25 °C. Experiments employed low excitation energy densities (~40 μJ cm^{-2} at 450 nm for dye **2** and ~23 μJ cm^{-2} at 550 nm for dye **3**), these excitation densities being selected to ensure matched densities of absorbed photons for both dyes, corresponding to ~0.6 absorbed photons/TiO_2 nanoparticle.

The recombination dynamics were monitored by observing the decay of the photoinduced cation absorption of the two dyes.[22] Typical data for the two sensitizer dyes are shown in Figure 3 employing probe wavelengths 610 and 720 nm for TiO_2 films sensitized dyes **2** and **3**, respectively. The decay traces shown in Figure 3 follow the formation of the dye cations according to reaction 1:

$$\mathrm{Dye} \xrightarrow{h\nu} \mathrm{Dye}^* \longrightarrow \mathrm{Dye}^+ + e^-_{\mathrm{TiO_2}} \quad (1)$$

and their recombination with photoinjected electrons according to reaction 2:

$$\mathrm{Dye}^+ + e^-_{\mathrm{TiO_2}} \longrightarrow \mathrm{Dye} \quad (2)$$

It is apparent that the recombination dynamics observed for dye **3** are significantly slower than those observed for dye **2**, exhibiting recombination half-times ($t_{50\,\%}$) of 300 and 4 μs, respectively. We attribute this retardation to an increase in the physical separation of dye cation from the metal oxide surface due to the insertion of the CD macrocycle. Consideration of the structures of two dyes **2** and **3** indicates an approximately 4 Å increase in the dye cation/TiO_2 separation for dye **3** compared to dye **2**. Assuming, as expected,[23] an exponential dependence of electron transfer rate upon spatial separation ($k_{et} \propto \exp(-\beta r)$, where $\beta = 1$–1.4 Å), this increase in spatial separation is consistent with the observed retardation of the charge-recombination dynamics.

It is apparent from Figure 3 that cyclodextrin encapsulation does not result in a significant reduction in the magnitude of the observed transient-absorption signal (with the initial amplitude actually being somewhat larger for dye **3**). Whilst pos-

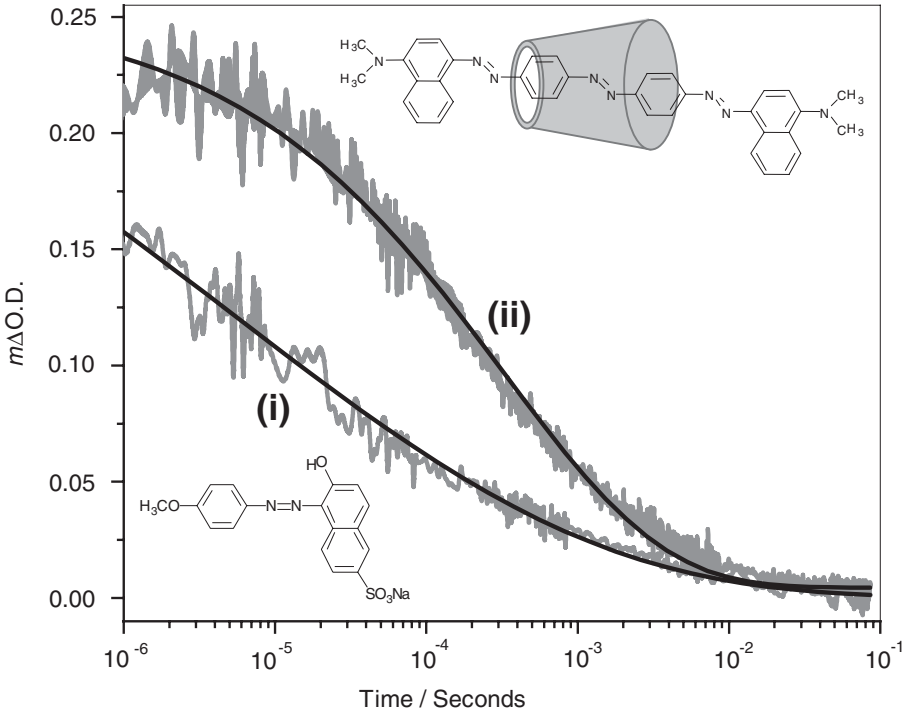

Figure 3. Transient-absorption data obtained for nanocrystalline TiO_2 films sensitized with dye **2** (curve i) and dye **3** (curve ii). The decay kinetics are assigned to the charge recombination of the photogenerated dye cations with the electrons in the trap/conduction band states in the TiO_2.

ADVANCED MATERIALS

sible differences in dye cation extinction coefficients preclude quantitative analysis, these data do indicate that encapsulation does not significantly reduce the yield of electron injection from the dye-excited state into the TiO_2 conduction band. This observation is consistent with the expected ultrafast nature of the electron-injection dynamics compared to the dye excited-state decay to ground, resulting in the electron injection yield being relatively insensitive to the insertion of an electron tunneling barrier layer between the dye and the TiO_2 surface, as we have discussed previously.[18]

It is apparent from the data shown in Figure 3 that temporal shape of the charge-recombination kinetics differs significantly between the two sensitizer dyes. For both dyes **2** and **3** the decay kinetics fit well to a stretched exponential function ($\Delta OD \propto \exp^{-(t/\tau)^{\alpha}}$) with $\alpha = 0.18$ and 0.37, respectively, as illustrated by the black lines in Figure 3. This shift is indicative with a transition from more transport-limited to more interfacial electron-transfer-limited recombination dynamics as the spatial separation of the dye cation from the TiO_2 surface is increased, consistent with our previous observations.[24]

In summary, we have demonstrated that cyclodextrin encapsulation of sensitizer dyes can be employed both to achieve the attachment of such dyes to nanocrystalline TiO_2 films, and to retard the interfacial charge-recombination dynamics of such films. Our approach is based upon insulation of the sensitizer dye at the molecular level. The slow charge-recombination kinetics observed for dye **3** most probably derives from a larger physical separation between the dye cation and TiO_2 film surface, consistent with the CD macrocycle resulting in a barrier to charge recombination. We note that this approach may also be suitable for controlling phase segregation and charge-recombination dynamics at organic/organic interfaces, and can furthermore be extended to encapsulation of organic polymers[15] for applications in polymer/inorganic and polymer organic heterojunctions. We conclude from the present findings that molecular encapsulation provides a versatile approach to control of interfacial charge transfer.

Experimental

Synthesis of Sensitizer Dyes: The cyclodextrin dye rotaxane was prepared following a modified version of a previously published procedure [17]. The formation of rotaxane structure was fully characterized using ^{1}H NMR and 2D COSY (correlated spectroscopy) techniques (see Supplementary information).

Synthesis of Nanocrystalline TiO_2 Films: The TiO_2 paste, consisting of 15 nm sized particles as determined by high-resolution transmission electron microscopy (HRTEM), were prepared from a sol–gel colloidal suspension containing 12.5 wt.-% TiO_2 particles and 6.2 wt.-% Carbowax 20 000. The nanoparticles were fabricated by the following procedure. 20 ml of titanium isopropoxide were injected into 5.5 g of glacial acetic acid under argon atmosphere and stirred for 10 min. The mixture was then injected into 120 mL of 0.1 M nitric acid under anhydrous atmosphere at room temperature in a conical flask and stirred vigorously. The flask was left uncovered and heated at 80 °C for 8 h. After cooling, the solution was filtered using a 0.45 μm syringe filter, diluted to 5 wt.-% TiO_2 by the addition of H_2O and then autoclaved at 220 °C for 12 h. The colloids were re-dispersed with a 60 s cycle burst from a LDU Soniprobe horn. The solution was then concentrated to 12.5 % on a rotary evaporator using a membrane vacuum pump at a temperature at 40 °C. 6.2 % by weight Carbowax 20 000 was added and the resulting paste was stirred slowly overnight to ensure homogeneity. The suspension was spread on the substrates by a glass rod, using 3M adhesive tapes as spacers. After the films were dried in air, they were sintered at 450 °C for 20 min in air. The thickness of the TiO_2 films was controlled using different tapes, resulting in film thicknesses of between 4 and 8 μm.

Laser-Based Transient-Absorption Spectroscopy: Transient-absorption studies of the dye-sensitized nanocrystalline films were conducted as detailed previously by covering the film with a 1:1 ethylene carbonate/propylene carbonate solution and glass cover slide. For determination of the transient-absorption data, samples were excited at 450 and 550 nm for dyes **2** and **3**, respectively, with pulses from a nitrogen-laser-pumped dye laser (< 1 ns pulse duration, 0.8 Hz, intensity, ~ 40 μJ cm^{-2} at 450 nm for dye **2** and ~ 23 μJ cm^{-2} at 550 nm for dye **3**), these excitation densities being selected to ensure matched densities of absorbed photons for both dyes, corresponding to ~ 0.6 absorbed photons/TiO_2 nanoparticle. The resulting photoinduced change in optical density was monitored by employing a 100 W tungsten lamp, with 20 nm bandwidth monochromators before and after sample, a homebuilt photodiode-based detection system and a TDS-220 Tektronix DSO oscilloscope. UV-visible measurements were performed after each experiment to monitor any desorption/degradation of the sensitizer dye. No changes in the UV-visible spectra were observed for the photoelectrodes after transient-absorption experiments.

Received: March 5, 2004

[1] B. O'Regan, M. Grätzel, *Nature* **1991**, *353*, 737.
[2] K. Janez, T. Marko, F. Smole, O. Krasovec, B. Orel, *Sol. Energy Mater. Sol. Cells* **2002**, *71*, 387.
[3] E. Topoglidis, J. C. Collin, E. Palomares, J. R. Durrant, *Chem. Commun.* **2002**, 1518.
[4] D. Ryan, S. N. Rao, H. Rensmo, D. Fitzmaurice, J. A. Preece, S. Wenger, J. F. Stoddart, N. Zaccheroni, *J. Am. Chem. Soc.* **2000**, *122*, 6252.
[5] L. Cusack, X. Marguerettaz, S. N. Rao, S. Nagaraja, J. Wenger, D. Fitzmaurice, *Chem. Mater.* **1997**, *9*, 1765.
[6] V. Shklover, Y. E. Ovchinnikov, L. S. Braginsky, S. M Zakeeruddin, M. Grätzel, *Chem. Mater.* **1998**, *10*, 2533.
[7] R. Huber, J. E. Moser, M. Grätzel, J. Wachtveitl, *Chem. Phys.* **2002**, *285*, 39.
[8] R. Huber, S. Spolein, J. E. Moser, M. Grätzel, J. Wachtveitl, *J. Phys. Chem. B* **2000**, *104*, 8995.
[9] M. R. Craig, M. G. Hutchings, H. L. Anderson, *Angew. Chem. Int. Ed.* **2001**, *40*, 1071.
[10] S. Anderson, H. L. Anderson, *Angew. Chem. Int. Ed. Engl.* **1996**, *35*, 1956.
[11] J. E. H. Buston, J. R. Young, H. L. Anderson, *Chem. Commun.* **2000**, 905.
[12] J. E. H. Buston, F. Marken, H. L. Anderson, *Chem. Commun.* **2001**, 1046.
[13] C. A. Stanier, S. J. Alderman, T. D. W. Claridge, H. L. Anderson, *Angew. Chem. Int. Ed.* **2002**, *41*, 1769.
[14] a) C. A. Stanier, M. J. O'Connell, W. Clegg, H. L. Anderson, *Chem. Commun.* **2001**, 493. b) C. A. Stanier, M. J. O'Connell, W. Clegg, H. L. Anderson, *Chem. Commun.* **2001**, 787.
[15] F. Cacialli, J. S. Wilson, J. J. Michels, C. Daniel, C. Silva, R. H. Friend, P. Severin, P. Samori, J. P. Rabe, M. J. O'Connell, P. N. Taylor, H. L. Anderson, *Nat. Mater.* **2002**, *1*, 160.
[16] J. S. Park, M. Srinivasarao, unpublished.
[17] S. Anderson, T. D. Claridge, H. L. Anderson, *Angew. Chem. Int. Ed. Engl.* **1997**, *36*, 1310.

[18] E. Palomares, J. N. Clifford, S. A. Haque, T. L. Lutz, J. R. Durrant, *J. Am. Chem. Soc.* **2003**, *125*, 475.
[19] Y. Tachibana, J. E. Moser, M. Grätzel, D. R. Klug, J. R. Durrant, *J. Phys. Chem.* **1996**, *100*, 20 056.
[20] S. A. Haque, Y. Tachibana, R. L. Willis, J. E. Moser, M. Grätzel, D. R. Klug, J. R. Durrant, *J. Phys. Chem. B* **2000**, *104*, 538.
[21] S. A. Haque, T. Park, A. B. Holmes, J. R. Durrant, *ChemPhysChem* **2003**, *1*, 89.
[22] The optical excitation of nanocrystalline TiO_2 sensitized by dyes **2** and **3** results in an instrument-response-limited appearance of a broad peaks at 610 and 720 nm, which we attribute to the radical cation bands of dye **2** and **3**, respectively.
[23] D. S. Bendall, *Protein Electron Transfer* (Eds: C. C. Moser, P. L. Dutton), BIOS Scientific Publishing, Abingdon, UK **1996**, Ch. 1.
[24] J. N. Clifford, G. Yahioglu, L. R. Milgrom, J. R. Durrant, *Chem. Commun.* **2002**, 1260.

Inorganic–Biomolecular Hybrid Nanomaterials as a Genetic Molecular Code System**

By *Jin-Ho Choy*,* *Jae-Min Oh*, *Man Park*, *Kwang-Min Sohn*, and *Jong-Won Kim*

Globalization along with rapid advances in various technologies inevitably require a highly confidential identification system that carries a high density of information and allows it to be reliably deciphered using a global criterion. Although there are currently many diverse kinds of coding systems, such as barcodes, watermarks, fingerprints, etc., none of them can satisfy the above requirement. In general, confidential systems such as watermarks carry no coded data to hamper universal adoption, while globalized systems such as barcodes provide no confidentiality, thus reducing their creditability. In addition, most of them are extremely vulnerable to forgery, meaning that crucial information can be manipulated or copied. Recently, a genetic code system using the base units of a DNA strand has been suggested as a possibility for overcoming this dilemma.[1–7] It is well known that a tremendous amount of reliable information can be incorporated into a short DNA strand without any concern about forgery. In spite of this fascinating feature, a genetic code system still remains at the concept stage, mainly due to the problems inherent with naked DNA strands, such as instability, flocculation, and difficult recovery. Here, we have attempted to establish a practical genetic code system by solving these problems and further systematizing a series of advanced concepts.

Nanohybridization has been employed to cope with these problems. First of all, unstable naked DNA strands (either single or double) were intercalated into an inorganic matrix—a layered double hydroxide (LDH)—to form a stable DNA–LDH nanohybrid.[8,9] These encapsulated DNA strands exhibit relatively good thermal stability (up to about 300 °C; Fig. 1a) and chemical resistance (stable at pH greater than 4). In addition, they can be recovered safely without any adverse effects by extracting with 0.01 M mineral acid, even after treatment with a DNase I/Tris(hydroxymethyl)aminomethane (Tris)–HCL buffer solution containing Ca^{2+}/Mg^{2+} ions for 2 h at 37 °C (Fig. 1b). These results indicate that the DNA strands intercalated into LDH are stable enough to endure severe physical and biological environments. Their dispersion ability is also guaranteed due to the small size of the LDH crystals. A scanning electron microscopy (SEM) study clearly showed that each hybrid crystal can be easily separated and mixed

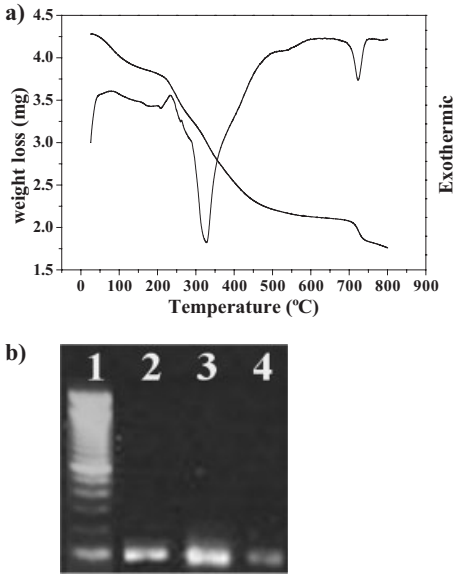

Figure 1. Stability of DNA–LDH against severe thermal and enzymatic surroundings. a) Thermogravimetry differential thermal analysis (TG-DTA) curve for DNA–LDH. The strong exothermic peak around 340 °C in the DTA curve represents thermal degradation of the DNA strands, which implies that they are safely preserved up to at least 300 °C due to the strong electrostatic stabilization between the DNA backbone and the LDH layer. b) The gel electrophoresis result for the PCR product of DNA recovered from DNA–LDH nanohybrid: lane 1: 100 base-pair ladder DNA; lane 2: positive control of 100 base-pair genetic code DNA; lane 3: DNA recovered from the DNA–LDH nanohybrid by acidification; lane 4: DNA recovered from the DNA–LDH nanohybrid after treatment in DNase I solution for 2 h. The clear DNA band at 100 base pairs shown in lanes 3,4 represents the safe preservation of DNA against extreme biological surroundings.

[*] Prof. J. H. Choy, Dr. J.-M. Oh, Prof. M. Park
National Nanohybrid Materials Laboratory (NNML)
School of Chemistry and Molecular Engineering
Seoul National University
151-747, Seoul (South Korea)
E-mail: jhchoy@plaza.snu.ac.kr
K. M. Sohn, Prof. J.-W. Kim
Department of Laboratory Medicine
Samsung Medical Center
School of Medicine, Sungkyunkwan University
50 Ilwon-dong, Kangnam-ku, Seoul, 135-710 (South Korea)

[**] This study was supported by the Korean Ministry of Science and Technology through the National Research Laboratory Program (1999) and National R&D Project for Nano Science and Technology, and in part by the Brain Korea 21 program. Supporting Information is available online from Wiley Interscience or from the author.

 DOI: 10.1002/adma.200400027